VI International Conference on Adaptive Modeling and Simulation
ADMOS 2013
J. P. Moitinho de Almeida, P. Díez, C. Tiago and N. Parés (Eds)

ON THE FEASIBILITY OF GOAL-ORIENTED ERROR ESTIMATION FOR SHIP HYDRODYNAMICS

JEROEN WACKERS, GANBO DENG AND MICHEL VISONNEAU

Laboratoire de recherche en Hydrodynamique, Energétique et Environnement Atmosphérique,
Ecole Centrale de Nantes, CNRS-UMR 6598, 44321 Nantes Cedex 3, France
e-mail: jeroen.wackers@ec-nantes.fr

Key words: Error Estimation, Anisotropic Refinement, High-Reynolds Flows

Abstract. An initial study is made of the possibilities for goal-oriented error estimation and anisotropic grid refinement in the simulation of water flow around ships. A finite-volume discretisation for the adjoint solution is presented together with least-squares computation of the local residuals. The paper shows the difficulties in the computation of adjoints and residuals for high-Reynolds flows, but indicates that error estimation and grid refinement for such flows may be possible.

1 INTRODUCTION

Goal-oriented flow simulation, for the purpose of this article, denotes simulation methods where numerical or physical parameters and techniques can be automatically adjusted by the solver in order to provide accurate and efficient computation of a given single output parameter. The concept originates from the idea that flow computations are often performed to answer a specific question and that computational resources should therefore be applied for answering this question, and for nothing else. And also, if non-expert users are to base crucial design decisions only on the results of CFD computations, they need simulation software which provides reliable results at least partially in an automatic way. Thus, goal-oriented simulation has two key aspects: the simulation has to be adaptive to provide efficient results and the precision of these results must be estimated to guarantee reliability. In this paper, we shall study both error estimation and adaptive grid refinement.

While adjoint-based error estimation and mesh refinement is common for the simulation of structures [1] and has been successfully applied to compressible Euler flow [5], its use for incompressible Reynolds-averaged Navier-Stokes flows at high Reynolds numbers is not straightforward and few results have been reported. Notably, Stück and Rung [8] use the adjoint solution for hull form optimisation. Particular difficulties for these flows are:

- The RANS equations contain turbulence models which are often not taken into account for the computation of the adjoint solution. This may have an influence on the quality of the error estimation.

- To model turbulent boundary layers, meshes are used with very high aspect-ratio cells near the walls. The adjoint equations and especially the evaluation of the local truncation error used in the error estimation are sensible to these meshes.

- The flow is incompressible, which is very hard for grid refinement. There are no obvious local zones which require great precision (such as shock waves and contact discontinuities in compressible flow); to get accuracy, the flow needs to be more or less well resolved everywhere. Finding the resulting optimum grid sizes requires a delicate balance which puts strong requirements on the quality of the refinement criterion.

The goal of this article is to provide an initial investigation of the possibilities for adjoint-based error estimation and grid refinement for the computation of water flow around ships. A continuous adjoint solver is under development for ISIS-CFD, the unstructured Navier-Stokes solver developed by ECN-CNRS. This solver is combined with local truncation error estimation by high-order integration of the RANS equations over the grid cells [4] for error estimation. In the light of the difficulties outlined above, these techniques are investigated critically. Grid refinement for the flows of interest and the unstructured hexahedral meshes that we use, is necessarily anisotropic [10]: grid cells to be refined can be divided in only one direction, as well as in several. For goal-oriented anisotropic refinement, we show a first test with an approximate implementation of the technique proposed by [5] where the criterion is based on the Hessians of the fluxes.

Section 2 describes the ISIS-CFD flow solver. Then section 3 introduces the continuous adjoint equations and briefly describes their discretisation. Sections 4 and 5 give, respectively, an overview of the error estimation and grid refinement techniques. Finally, section 6 shows initial tests on laminar and turbulent flows which shed some light on the possible efficiency of these methods.

2 THE ISIS-CFD FLOW SOLVER

ISIS-CFD, available as a part of the FINE^{TM}/Marine computing suite, is an incompressible unsteady Reynolds-averaged Navier-Stokes (RANS) method [3, 7]. The solver is based on the finite volume method to build the spatial discretisation of the transport equations. Pressure-velocity coupling is obtained through a Rhie & Chow SIMPLE-type method: in each time step, the velocity updates come from the momentum equations and the pressure is given by the mass conservation law, transformed into a pressure equation.

The discretisation is face-based. While all unknown state variables are cell-centered, the systems of equations used in the implicit time stepping procedure are constructed face by face. Fluxes are computed in a loop over the faces and the contribution of each face is

then added to the two cells next to the face. This technique poses no specific requirements on the topology of the cells. Therefore, the grids can be completely unstructured, cells with an arbitrary number of arbitrarily-shaped faces are accepted. The code is fully parallel using the MPI (Message Passing Interface) protocol.

An automatic adaptive grid refinement technique is included in the solver ISIS-CFD [9, 10]. The method supports the isotropic and anisotropic refinement of unstructured hexahedral meshes. Earlier refinements can be undone in order to adapt the grid to unsteady problems. The refinement criterion, which indicates where the grid must be refined, can be modified very easily; different refinement criteria have already been tested. And finally, the grid refinement is performed in parallel and includes an automatic dynamic load balancing in order to redistribute the refined grid over the processors when some partitions have been refined more than the others.

3 ADJOINT EQUATIONS AND DISCRETISATION

This section discusses briefly the adjoint to the incompressible RANS equations and its discretisation. The RANS system of equations itself, $\mathcal{N}(\mathbf{U}) = 0$ can be expressed as follows:

$$\left[u_i u_j + p\delta_{i,j} - \mu\left((u_i)_j + (u_j)_i\right)\right]_j = 0, \tag{1a}$$

$$(u_j)_j = 0, \tag{1b}$$

with u_i the velocity components, p the pressure, μ the (variable) viscosity coming from a turbulence model, and δ the Kronecker delta function. The Einstein summation convention is used, indices outside brackets denote differentiation. $\mathbf{U} = [u_1, u_2, u_3, p]^T$ is the exact solution of this system. Finally, $\mathbf{U}_h$ denotes an approximate (numerical) solution of (1).

We are interested in the error for an output functional on the solution $J(\mathbf{U})$, when it is computed from $\mathbf{U}_h$ instead of $\mathbf{U}$. Linearisation gives:

$$J(\mathbf{U}_h) - J(\mathbf{U}) \approx (\mathbf{g}, \mathbf{U}_h - \mathbf{U})_\Omega, \qquad \text{with } \mathbf{g} = [\frac{\partial J}{\partial u_1}, \frac{\partial J}{\partial u_2}, \frac{\partial J}{\partial u_3}, \frac{\partial J}{\partial p}]. \tag{2}$$

$(\cdot, \cdot)_\Omega$ denotes an inner product, integrated over the flow domain. The adjoint solution $\mathbf{z}$ is then defined by:

$$(\mathbf{z}, \mathcal{N}(\mathbf{U}_h) - \mathcal{N}(\mathbf{U}))_\Omega = (\mathbf{g}, \mathbf{U}_h - \mathbf{U})_\Omega, \qquad \forall(\mathbf{U}_h - \mathbf{U}). \tag{3}$$

For the RANS equations, the adjoint system reads:

$$-u_i(z_j)_i - u_i(z_i)_j + (z_p)_j - \mu\left((z_i)_j + (z_j)_i\right)_j = g_j, \tag{4a}$$

$$(z_j)_j = g_p, \tag{4b}$$

where $\mathbf{z} = [z_1, z_2, z_3, z_p]^T$.

Like the primal system, the adjoint equations are discretised with a finite-volume technique and a segregated Rhie & Chow method; this is possible because the continuity equation (4b) is the same as in the primal system. Space is lacking here to describe the discretisation in full, but a few remarks are given:

- The term $-u_i(z_i)_j$ makes these equations non-conservative and impossible to put in conservative form. Therefore, the standard finite-volume technique where the equations are integrated over the cells to produce expressions containing only the fluxes over the cell faces, cannot be used. To construct a finite-volume like discretisation, we use constant cell-centred values for the velocities u_i when integrating over a cell. Thus, for all convective terms, the fluxes over a face are different for the left and right cells, since the u_i on the two sides of the face are different.

- The convective term $-u_i(z_j)_i$ is discretised with upwind reconstruction. However, the term $-u_i(z_i)_j$ originates from the linearisation of the mass fluxes which, in the primal system, use the Rhie & Chow reconstruction that is closer to the central discretisation. We found that, for the adjoint system to be stable, also the adjoint terms $-u_i(z_i)_j$ require a central discretisation. Despite this discretisation, the current formulation lacks robustness for high-Reynolds flows in regions of very low velocity, where iterative errors sometimes increase very slowly leading to an eventual divergence of the computation. This is a problem which could come either from the discretisation or from the segregated solution procedure; we are working on its solution.

- The velocities in the convective operators are the velocities u_i coming from the primal system, but due to the minus signs in (4a) the adjoint 'flow' is backwards. This must be taken into account in the upwind discretisations.

As for the primal system, the z_i-equations are solved with Gauss-Seidel while PGCStab is used for the z_p-equation. The z_i-corrections are underrelaxed, but not the z_p-correction.

4 ESTIMATING RESIDUALS

Equation (3) can be used directly to estimate the error in $J(\mathbf{U}_h)$ or even to obtain an improved approximation by subtracting the error estimation from the computed value of J. For this, besides the adjoint solution, we need to compute the residuals $\mathcal{N}(\mathbf{U}_h)$, the result of applying the exact RANS equations to the approximate numerical solution. Since we cannot evaluate these exact equations, the residuals are approximated with a higher-order finite-volume discretisation, similar to [4]. This approximation, valid on structured and unstructured grids, is performed as follows:

- Flux vectors in the face centres and in the nodes of the faces are computed with least-squares polynomials. For each node, third-order polynomials for each component

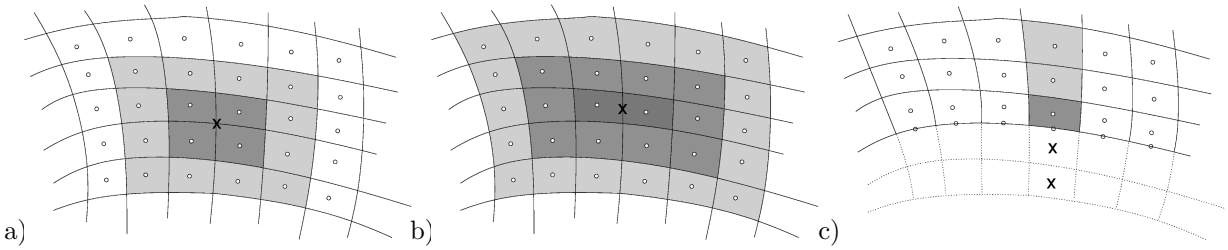

Figure 1: Stencils used in the residual estimation, for reconstruction in nodes (a), face centres (b), and for extrapolating two layers of ghost cells on the boundary (c). Examples on structured grids.

of U_h are fitted through the values in the neighbour cells of the nodes and the neighbours' neighbours (figure 1a). For the faces, the two cells next to the face are used as well as their neighbours and neighbours' neighbours (figure 1b). These are the minimum stencil sizes which ensure that sufficient points are available for fitting third-order polynomials, i.e. four points in all directions. From these fitted polynomials, we get the state vector and derivatives in the nodes and face centres, which are used to compute fluxes.

- Then, third-order accurate quadrature integration of the flux over the faces is performed with the face centre and nodal values. In 2D, third-order accuracy is obtained by assigning a weight of $\frac{2}{3}$ to the face and $\frac{1}{6}$ to each of the two face nodes. Weighting coefficients for arbitrary faces in 3D are under study.

Since the least-squares polynomials are fourth-order accurate, the resulting finite-volume approximation of $\mathcal{N}(\mathbf{U}_h)$ is at least third-order accurate for the convection (which involves one differentiation) and second-order for the diffusion (which requires two differentiations). This is an order more than the primary discretisation of ISIS-CFD, so it is sufficient. Theoretically, the same order of accuracy can be obtained more easily by fitting third-order polynomials through the cell centres and extracting first and second derivatives from these polynomials, which are then substituted directly in (1) to find the residuals. In practice, we have found that this alternative procedure is less accurate so it is not used.

Finally, tests on manufactured solutions revealed strong errors near curved boundaries with large aspect-ratio cells, which are typical for high-Reynolds flows. These errors appear because the cells on the surface are missing the neighbours' neighbour cells in the wall direction; they can be reduced by using symmetric stencils for the least-squares fits, even in the boundary cells. To obtain these, two layers of ghost cells are created at the boundaries whose values are set by extrapolation using 1D third-order polynomials fitted to three cell values and the known value on the face (figure 1). These ghost cells are then used like standard cells for the reconstruction in the nodes and faces. While no new information is added through the extrapolation, this procedure significantly reduces the errors near boundaries.

5 GOAL-ORIENTED REFINEMENT

Apart from error estimation, the adjoint solution can be used for grid refinement. A straightforward way to do this would be to use the local integrand $\mathbf{z} \cdot (\mathcal{N}(\mathbf{U}_h) - \mathcal{N}(\mathbf{U}))$ from equation (3) as a refinement criterion. However, this expression is a scalar so it cannot be used for anisotropic grid refinement, as it cannot specify different cell sizes in different directions.

A method for anisotropic grid refinement which is suitable for our metric-tensor refinement criteria [10] is presented by Loseille et al. [5] for the Euler equations. They express the local residuals in terms of projection errors for the fluxes. Using this, they show that these projection tensors can be minimised if a refined mesh is based on metric tensors that are the Hessian matrices of second spatial derivatives of the flux components. The optimum mesh for computing J is obtained by weighting these Hessians with the gradients of the adjoint solution.

Loseille et al. show excellent results for their method applied to compressible Euler flow. We have made an approximate implementation of this method for RANS flows: the viscous terms are added to the fluxes without further analysis, while separate treatment is advised [2]. For the computation of the flux Hessians, we use third-order cell-centred polynomials which are least-squares fitted to the fluxes computed in the cell centres. An initial test for RANS will be presented in the next section.

6 NUMERICAL TESTS

6.1 Error estimation for 2D profiles

The quality of the adjoint error estimation is tested with two 2D wing section test cases. The first, laminar case is the NACA0012 profile at 4° angle of attack and $Re = 1000$. Turbulent flow is computed around the Nakayama B profile [6] at 4° angle of attack and $Re = 1.2 \cdot 10^6$. Adjoints are computed for two functionals: the drag force and the integral of u_1 over a rectangle in the wake, which resembles the evaluation of the propeller plane flow. The rectangle is centred at $[0.9, -0.02]$ and has dimensions 0.02×0.04 for the NACA wing and 0.01×0.02 for Nakayama. The computed functionals are corrected with the estimated error in order to improve the estimate.

For both cases, computations have been performed on structured C-topology and unstructured HEXPRESS grids with low-Reynolds boundary layers. Figure 2 gives an impression of the solutions. While the boundary layer is of course much thinner for the turbulent case, both flows are similar. No particular problems were encountered for the computation of the primal and the adjoint solutions. However, the computations of the residuals have significant errors near the walls (section 4). Also, the evaluation of the disk integral is complicated because the meshes are not specially refined in the disk zone, so on the coarser structured grids there were too few cells in the disk to perform the integration.

Computed and corrected functional values are given in figure 3. The adjoint error estimation is based on linearisation (section 3) so it is only valid near the asymptotic

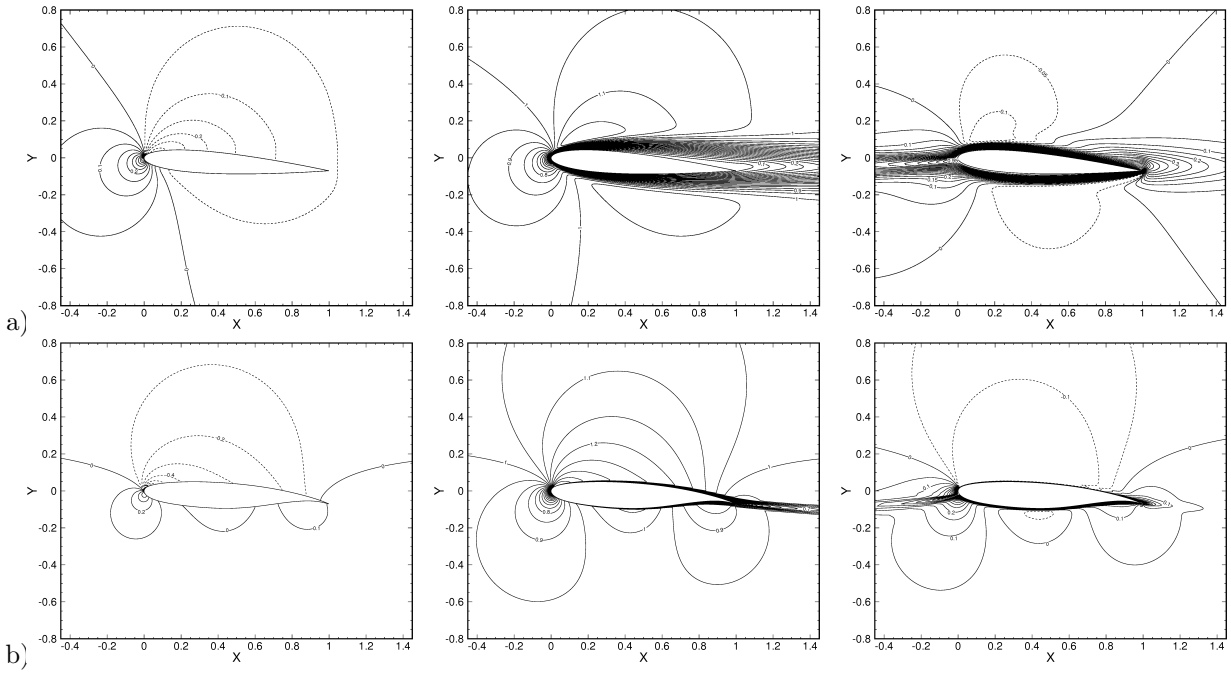

Figure 2: Flow around the NACA0012 (a) and Nakayama B (b) airfoil: pressure, horizontal velocity, and z_1 for the drag functional.

range. True asymptotic convergence is only reached for the NACA0012 drag functional on structured meshes; here the correction seems to improve the solution on the finer meshes even though the influence of near-wall errors in the residuals is non-negligible. Also for the turbulent Nakayama case, improvement may be obtained on the two finest meshes despite the catastrophic failure on the coarser meshes. On unstructured meshes in the laminar case, the error is systematically overestimated by a factor two. And while the solution is not improved for the turbulent case, the estimation is of the same order as the numerical error.

For the rectangle integral, the solutions are not in the asymptotic range so it is difficult to say whether the solutions are improved by the correction or not. However, also here the magnitude of the corrections is the same as the difference between the solutions.

In conclusion, it seems unrealistic to improve functional computations by error correction. However, the adjoint technique might be useful as an error estimator, certainly if the reliability of the residual computation is further improved.

6.2 Goal-oriented grid refinement for the KVLCC2

As an initial test of adjoint-based refinement, we compute the flow without free-surface effects around the KVLCC2 tanker at model scale, $Re = 6.4 \cdot 10^6$, (see figure 4). The turbulence model is EASM without rotation correction [3]. The refinement criterion consists of the flux Hessians, weighted by the gradients of the adjoint solution (section 5).

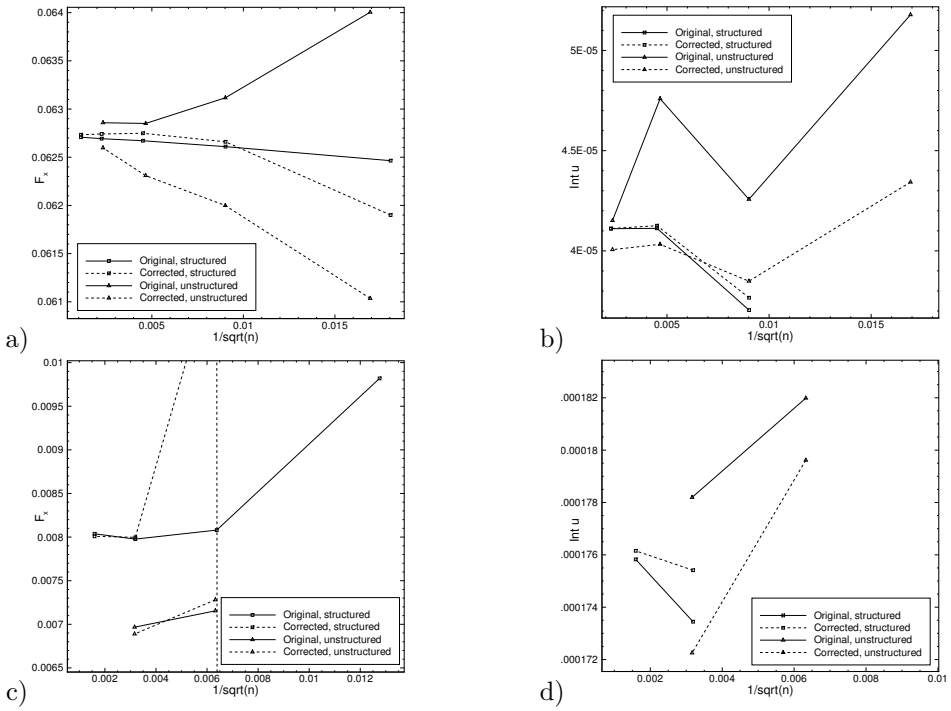

Figure 3: Original and corrected functionals for the NACA0012 airfoil: drag (a) and rectangle integral (b); for the Nakayama B airfoil: drag (c) and rectangle integral (d).

To prevent the divergence of the adjoint solver in low-velocity regions (section 3) which increases on finer grids, the adjoint solution is computed on the original coarse grid (265k cells), based on the converged primal solution for this grid. Automatic refinement is then performed in several steps until the solution and the mesh are converged; for these steps the flux Hessians are computed on the refined grid but the original adjoint solution is kept. In the future, we plan to compute also the adjoint solution on the refined mesh. The final mesh has about 1M cells, an automatic procedure in the solver was used to adjust the threshold for the criterion in order to obtain this number of cells.

The functional is the integral of the axial velocity over the propeller disk with (non-dimensional) radius 0.01541 and thickness 0.01, centered at x/L=0.0175 and z/L=-0.04688. This functional is chosen due to its importance for propeller design, however it does not guarantee that all flow details in the propeller plane are well captured: only the integral value has to be right!

The flow solution is presented in figure 5 and compared with a reference solution

Figure 4: Hull of the KVLCC2 tanker, with the stern facing left and the propeller plane indicated.

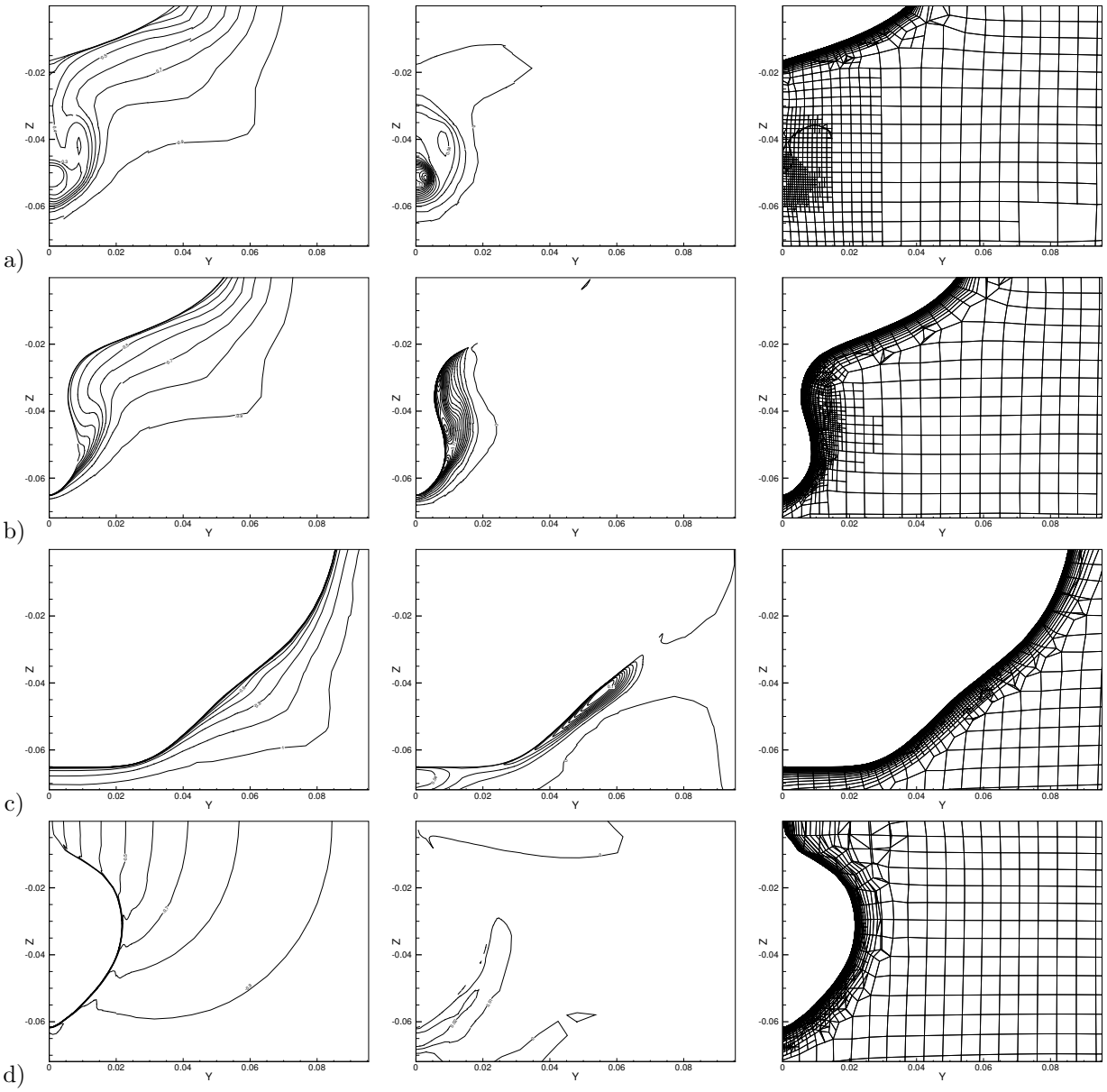

Figure 5: Goal-adaptive refinement for the KVLCC2: axial velocity, z_1 for the propeller plane functional, and the refined mesh in x-cross sections at the propeller plane $x/L = 0.0175$ (a), $x/L = 0.05$ (b), $x/L = 0.17$ (c), and near the bow at $x/L = 1.0$ (d).

Table 1: Computed values of the disk integral functional for the KVLCC2 test case.

Refined grid	Original grid	Reference fine grid
$-3.141 \cdot 10^{-6}$	$-2.621 \cdot 10^{-6}$	$-3.053 \cdot 10^{-6}$

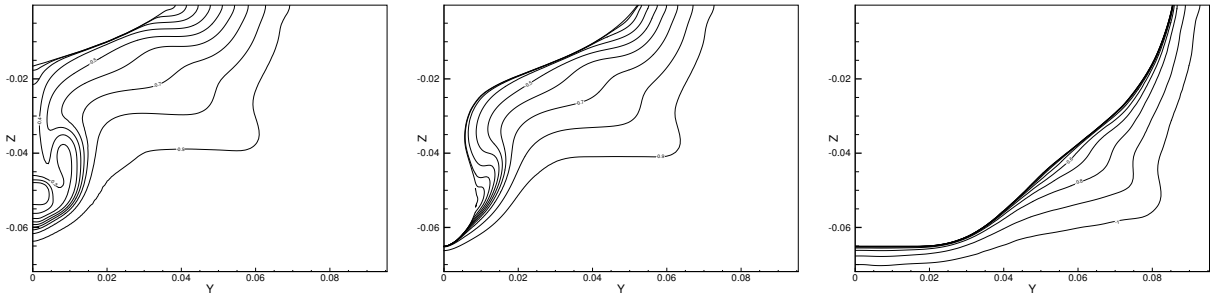

Figure 6: KVLCC2 reference fine grid solution: axial velocity at the propeller plane $x/L = 0.0175$, $x/L = 0.05$, and $x/L = 0.17$.

obtained on a very fine non-adapted grid (7M cells, figure 6). We see how the adjoint solution on the refined grid is non-uniform in the propeller plane, then gets high values around the rear of the ship and continues upstream at the ship's side. Near the bow it has diminished but it is still noticeable. This is reflected in the refined grid, which has fine cells mainly in the boundary layer region. Compared with refined grids created using a pressure Hessian criterion (see [9, 10]) the refinement is concentrated very close to the ship. Also, of course, there is little refinement at the front of the ship, although some refinement below the hull is visible in figure 5d.

The velocity profile in the propeller plane contains the correct 'hook' shape of low velocity around $y/L = 0.01$, $z/L = -0.04$, even though this hook is less noticeable than for the reference solution. Note that, according to the adjoint solution, the flow near the propeller hub has a much bigger influence on the integral than the hook. Further upstream, the velocity in the boundary layer is well resolved, but the velocity away from the hull is only computed approximately, since this velocity is unimportant for the integral according to the adjoint solution. The value of the disk integral functional is computed well (table 1), it is much closer to the fine-grid solution than the value computed on the original coarse grid without refinement. Thus, despite the difficulties in the computation of the adjoint, this initial result is promising.

7 CONCLUSION

This paper investigates the use of goal-oriented error estimation and adaptive grid refinement for high-Reynolds incompressible RANS flows. Error estimates and corrections for a functional are obtained by weighing the local residuals with an adjoint solution to the RANS equations. Tests on 2D airfoils show that it is probably unrealistic to improve

computed functionals by adding the error estimate, but that the estimations are of the same order as the actual errors and could thus be used as error estimators. Notable difficulties are the evaluation of the residuals near walls and the correction of functionals that are far away from asymptotic convergence.

An example is shown of anisotropic grid refinement based on the weighing of flux Hessians with the gradient of the solution. Whether this is the optimal choice for goal-oriented refinement and whether significant gains in efficiency can be made with respect to non goal-oriented grid refinement, remains to be investigated.

REFERENCES

[1] D. Aubry, P. Díez, B. Tie, and N. Parés. *Proceedings of the V International Conference on Adaptive Modelling and Simulation (ADMOS 2011)*, Paris, France (2011).

[2] A. Dervieux, A. Belme, H. Alcin, and F. Alauzet. Goal-oriented mesh adaptation for vortex shedding flows. *Proceedings of ECCOMAS 2012*, Vienna, Austria (2012).

[3] R. Duvigneau, M. Visonneau, and G.B. Deng. On the role played by turbulence closures in hull shape optimization at model and full scale. *J Mar Sci Techn* (2003) **8**(1):1–25.

[4] A. Hay and M. Visonneau. Error estimation using the error transport equation for finite-volume methods and arbitrary meshes. *Int J Comput Fluid Dyn* (2006) **20**(7):463–479.

[5] A. Loseille, A. Dervieux, and F. Alauzet. Fully anisotropic goal-oriented mesh adaptation for 3D steady Euler equations. *J Comput Phys* (2010) **229**:2866–2897.

[6] A. Nakayama. Characteristics of the flow around conventional and supercritical airfoils. *J Fluid Mech* (1985) **160**:155–179.

[7] P. Queutey and M. Visonneau. An interface capturing method for free-surface hydrodynamic flows. *Comput Fluids* (2007) **36**(9):1481–1510.

[8] A. Stück, T. Rung. Adjoint RANS with filtered shape derivatives for hydrodynamic optimisation. *Comput Fluids* (2011) **47**(1):22–32.

[9] J. Wackers, G.B. Deng and M. Visonneau. Tensor-based grid refinement criteria for ship flow simulation. *Proceedings of the 12th Numerical Towing Tank Symposium (NuTTS '10)*, Duisburg, Germany (2010).

[10] J. Wackers, G.B. Deng, A. Leroyer, P. Queutey, and M. Visonneau. Adaptive grid refinement for hydrodynamic flows. *Comput Fluids* (2012) **55**:85–100.